

REFERENCES

- Alexandre, M., and Dubois, P. (2000) Polymer-layered silicate nanocomposites: preparation, properties and uses of a new class of materials. Materials Science and Engineering, 28, 1-63.
- Connor, P., and Ottewill, R.H. (1971) Journal of Colloid and Interface Science, 37, 642.
- García-López, D., Picazo, O., Merino, J.C., and Pastor, J.M. (2003) Polypropylene-clay nanocomposites: effect of compatibilizing agents on clay dispersion. European Polymer Journal, 39, 945-950.
- Greenland, D.J., and Quirk, J.P. (1962) Proceedings of the Ninth National Conference on Clays and Clay Minerals. New York: Pergamon Press.
- Hasegawa, N., Kawasumi, M., Kato, M., Usuki, A., and Okada, A. (1998). Preparation and mechanical properties of polypropylene-clay hybrids using a maleic anhydride-modified polypropylene oligomer. Journal of Applied Polymer Science, 67, 87-92.
- Jaynes, W.F., and Boyd, S.A. (1991) Soil Science Society of America Journal, 55, 43.
- Kawasumi, M., Hasegawa, N., Kato, M., Usuki, A., and Okada, A. (1997) Preparation and mechanical properties of polypropylene-clay hybrids. Macromolecules, 30, 6333-6338.
- Lee, J.Y., and Lee, H.K. (2004) Characterization of organobentonite used for polymer nanocomposites. Materials Chemistry and Physics, 85, 410-415.
- Liu, X., and Wu, Q. (2001) PP/clay nanocomposites prepared by grafting-melt intercalation. Polymer, 42, 10013-9.
- Oriakhi, C. (1998) Nano sandwiches. Chemistry in Britain, 34, 59-62.
- Pérez-Santano, A., Trujillano, R., Belver, C., Gil, A., and Vicente, M.A. (2005) Effect of the intercalation conditions of a montmorillonite with octadecylamine. Journal of Colloid and Interface Science, 284, 239-244.
- Thaijaroen, W. (2000) Preparation and mechanical properties of NR/clay nanocomposite. M.S. Thesis, The Petroleum and Petrochemical College, Chulalongkorn University, Bangkok, Thailand.

- Usuki, A., Kato, M., Okada, A., and Kurauchi, T. (1997) Synthesis of polypropylene-clay hybrid. Journal of Applied Polymer Science, 63, 137-138.
- Vaia, R.A., Teukolsky, R.K., and Giannelis, E.P. (1994) Interlayer structure and molecular environment of alkylammonium layered silicates. Chemistry of Materials, 6, 1017-1022.
- Xi, Y., Ding, Z., He, H., and Ray, L.F. (2004) Structure of organoclays—an X-ray diffraction and thermogravimetric analysis study. Journal of Colloid and Interface Science, 277, 116-120.
- Yan, H., Chen, G., and Han, B. (1998) Interaction of cationic surfactants with iron and sodium montmorillonite suspensions. Journal of Colloid and Interface Science, 201, 158-163.
- Zhang, Y.-Q., Lee, J., Jang, H., and Nah, C. (2004) Polypropylene-clay nanocomposites prepared by in situ grafting-intercalating in melt. Composites Science and Technology, 64, 1383-1389.

APPENDICES

Appendix A CEC Values of Nanoclays

Cation exchange capacities (CEC) of nanoclays are determined by exchanging their surface cation with methylene blue. Dried nanoclay 2.0 g were dispersed in distilled water 300 ml. The suspension was stirred until a uniform dispersion was obtained. The pH value was adjusted in a range of 2.5-3.8 by sulfuric acid. The suspension was stirred for 15 min. Methylene blue solution (0.01 normal) was added slowly by buret into the clay slurry, while it was maintained a constant stirring. A drop of the suspended solution was placed on a filter paper to determine the end point. The end point was indicated by a formation of light blue halo around the drop. Adding methylene blue was continuous until the end point was obtained. After the end point was reached, the suspension was stirred for 2 min and retested for the end point.

The methylene blue index was calculated from equation (1)

$$MBI = \frac{E \cdot V \cdot 100}{W} \quad (1)$$

Where:

- MBI = methylene blue index for the clay (meq/100g of clay),
- E = concentration of methylene blue (meq/ml),
- V = amount of methylene blue required for titration (ml), and
- W = weight of dried nanoclay (g)

CEC values of nanoclays shows in Table A1

Table A1 Cation exchange capacity (CEC) values of nanoclays

Nanoclay	MMT(Kunipia F [®])	BEN(Mac-Gel [®] wn-02)
CEC (meq/100g)	115.50	52.55

Appendix B Impurities in Nanoclays

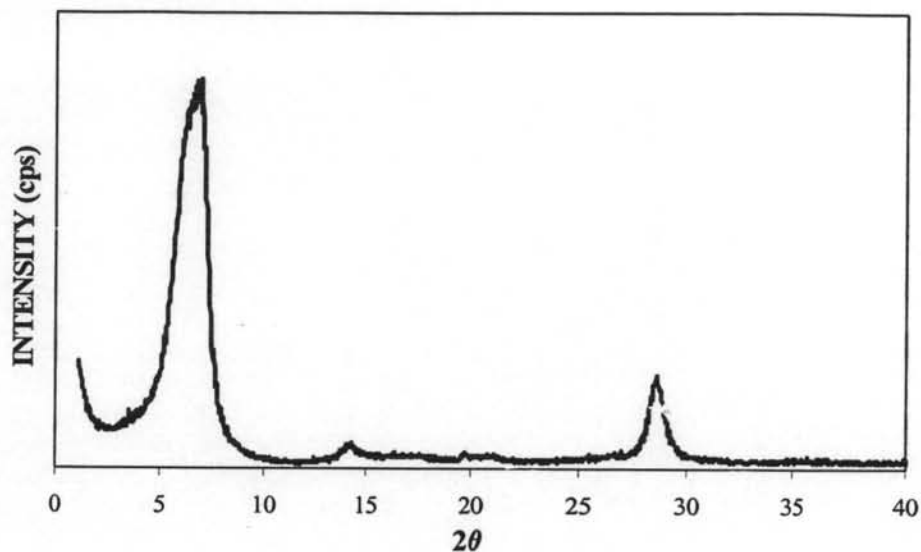


Figure B1 XRD pattern of montmorillonite.

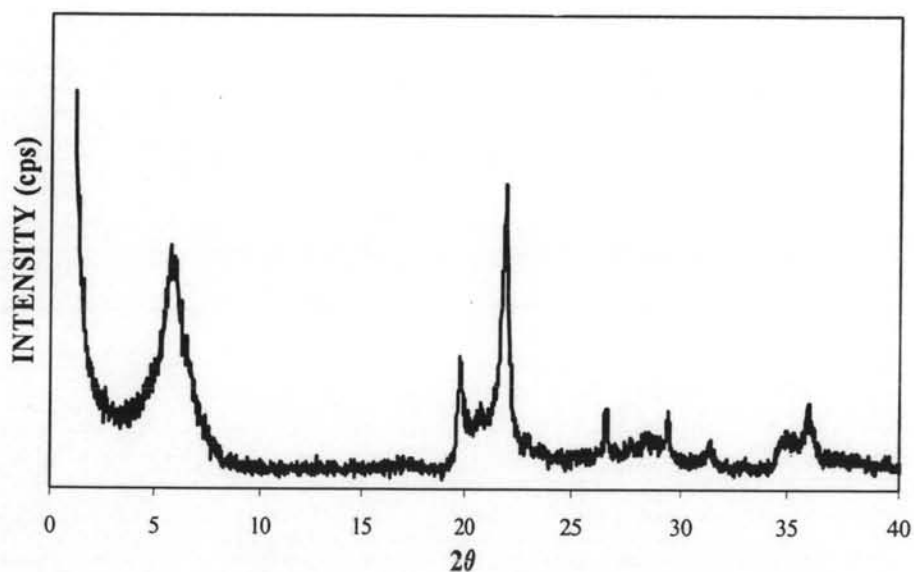


Figure B2 XRD pattern of bentonite.

From Figures B1 and B2, The XRD curve of bentonite appeared many peaks in range of 20-40 deg. This result indicates that there were many impurities as saponite, quartz, calcite, etc in bentonite.

Table B1 Component of bentonite

Component	Content (%)
Montmorillonite	28.87
Saponite,	16.26
Quartz	9.65
Calcite	8.25
Others	36.97

Appendix C Calculation

Content of Surfactant

Content of surfactant was calculated from equation (2)

$$\text{Content of surfactant (g)} = \frac{1.5 * \text{CEC} * 10^{-3} * W * M_w}{A} \quad (2)$$

Where:

- CEC = CEC of nanoclay (meq/100g of clay),
 W = weight of dried nanoclay (g),
 M_w = molecular weight of surfactant, and
 A = active ingredient of surfactant (%)

Example:

$$\begin{aligned} \text{Content of SA (g)} &= \frac{1.5 * 52.55 * 10^{-3} * 10 * 267}{90} \\ &= 2.3385 \text{ g} \end{aligned}$$

10 g bentonite was organomodified by 2.3385 g SA.

Content of HCl (only amine type)

Content of HCl was calculated from equation (3)

$$\text{Content of HCl (ml)} = \frac{3 * \text{CEC} * W}{C * 100} \quad (3)$$

Where:

- CEC = CEC of nanoclay (meq/100g of clay),
 W = weight of dried nanoclay (g), and
 C = concentration of HCl (M)

Example:

$$\begin{aligned} \text{Content of HCl (ml)} &= \frac{3 * 52.55 * 10}{11.96 * 100} \\ &= 1.318 \text{ ml} \end{aligned}$$

1.318 ml HCl was added for organomodified 10 g bentonite with 2.3385 g SA.

Content of Co-Intercalation Monomer (MAA)

Content of MAA was calculated from equation (4)

$$\text{Content of MAA (ml)} = \frac{0.5 * \text{CEC} * 10^{-3} * W * M_w}{D * A} \quad (4)$$

Where:

- CEC = CEC of nanoclay (meq/100g of clay),
 W = weight of dried nanoclay (g),
 M_w = molecular weight of MAA,
 D = density of MAA (g/ml), and
 A = active ingredient of surfactant (%)

Example:

$$\begin{aligned} \text{Content of SA (g)} &= \frac{0.5 * 52.55 * 10^{-3} * 10 * 86.09}{1.010 * 99.5} \\ &= 0.450 \text{ ml} \end{aligned}$$

0.450 ml MAA was added for modified 10 g organo-BEN.

Appendix D Condition of Ion Exchange Reaction

Bentonite was organomodified with hexadecyltrimethylammonium chloride in various condition of ion exchange reaction. Adding acid (hydrochloric acid) was various (3CEC, 1.5CEC, and 0CEC). The basal spacing of organo-BENs were determined by XRD (Tale C1)

Table D1 The basal spacing of organo-BENs in various condition of ion exchange reaction

Condition	3CEC	1.5CEC	0CEC
Basal spacing (Å)	22.07	24.79	28.849

The highest basal spacing was 0CEC. Organomodified bentonite with quaternary ammonium salt, adding acid was not necessary to protonation unlike amine.

Appendix E Properties of PP and PP-PP/DCP

Table E1 Properties of PP and PP-PP/DCP

Properties	PP	PP-PP/DCP
T _c (°C)	106.3	108.8
T _m (°C)	156.4	156.4
ΔH _{DSC} (J/g)	57.189	61.573
%Crystallinity	27.36	29.49
T _d (°C)	452.4	422.4
MFI (g/10 min)	10.80 (0.14)*	24.67 (0.14)*
Tensile strength (MPa)	35.94 (0.17)*	35.22 (0.45)*
Tensile modulus (MPa)	2068.59 (61.73)*	1915.56 (47.47)*
Strain at break	189.35 (47.26)*	395.93 (38.50)*

()* : standard derivation

Appendix F Raw Data

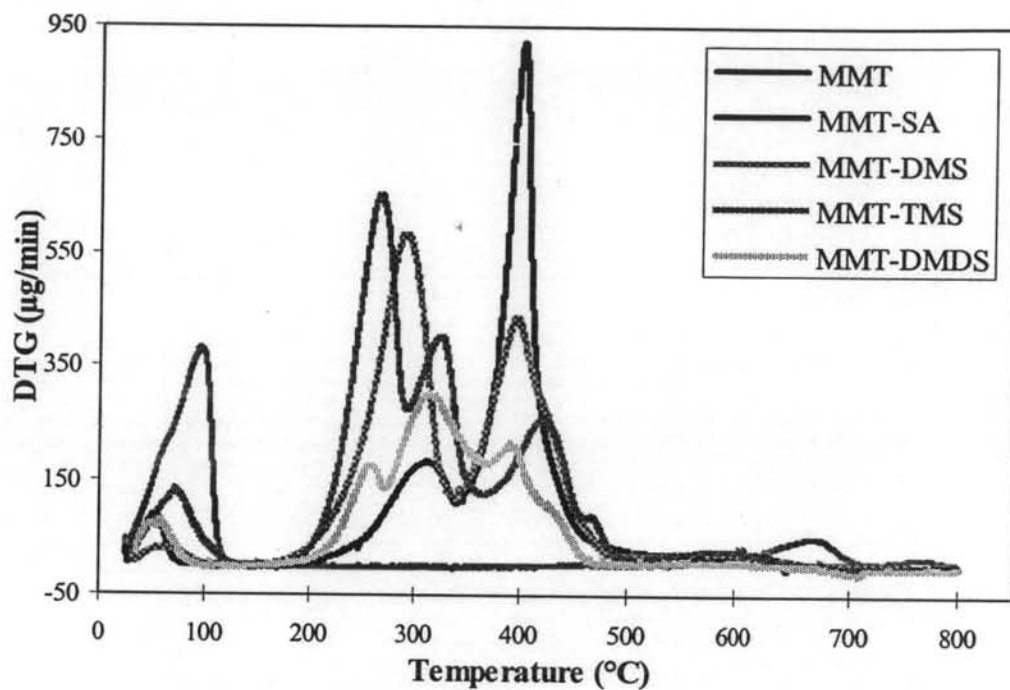


Figure E1 DTG thermograms of organo-MMTs.

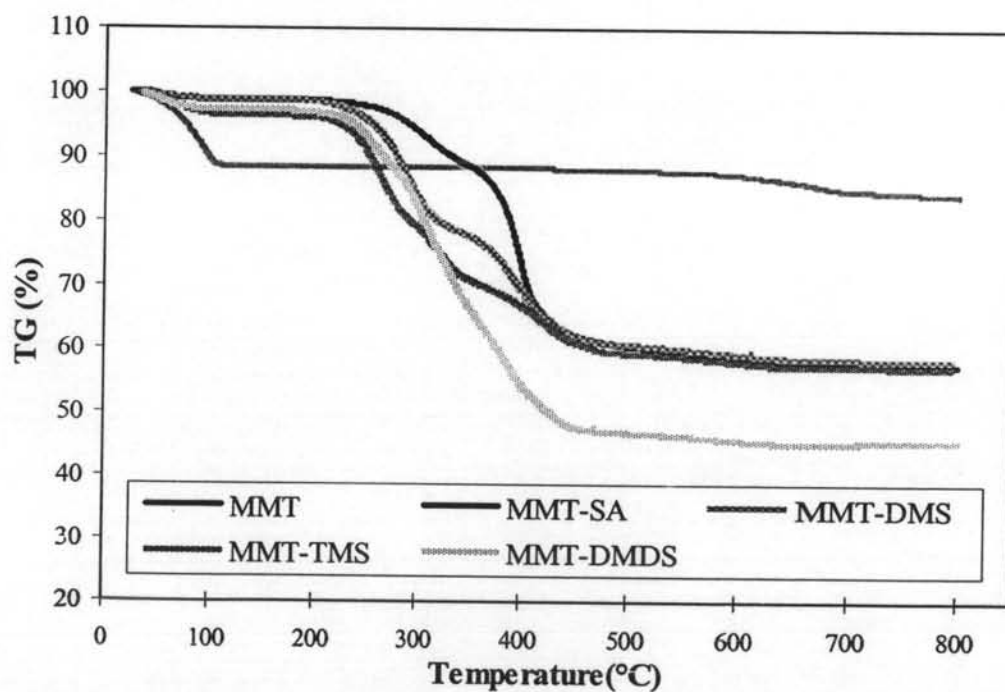


Figure E2 TG thermograms of organo-MMTs.

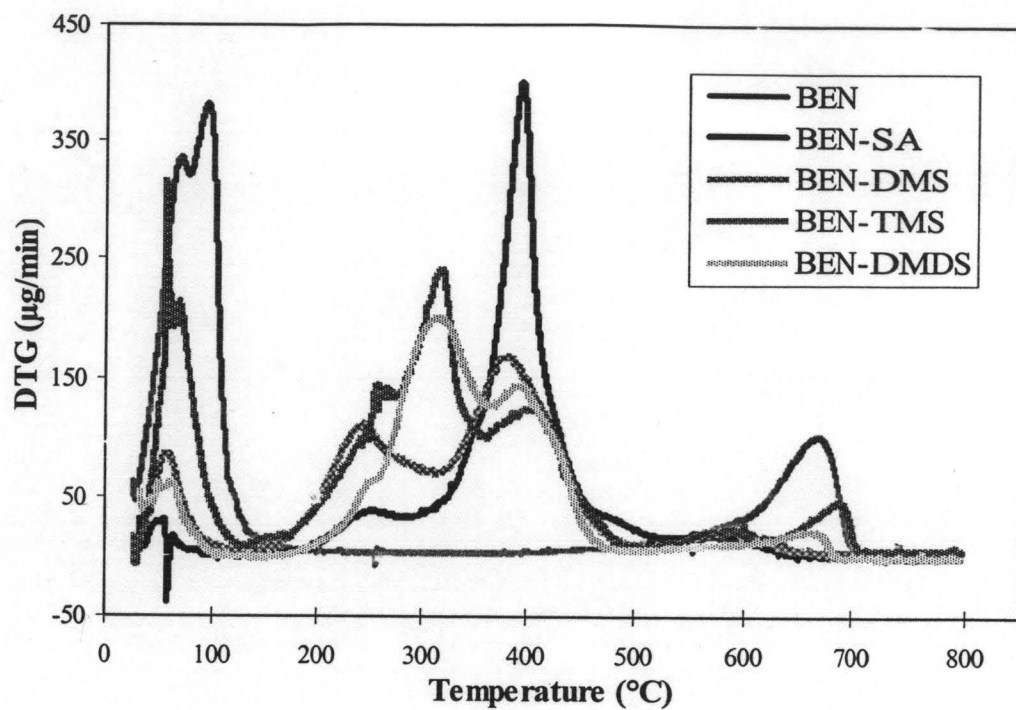


Figure E3 DTG thermograms of organo-BENs.

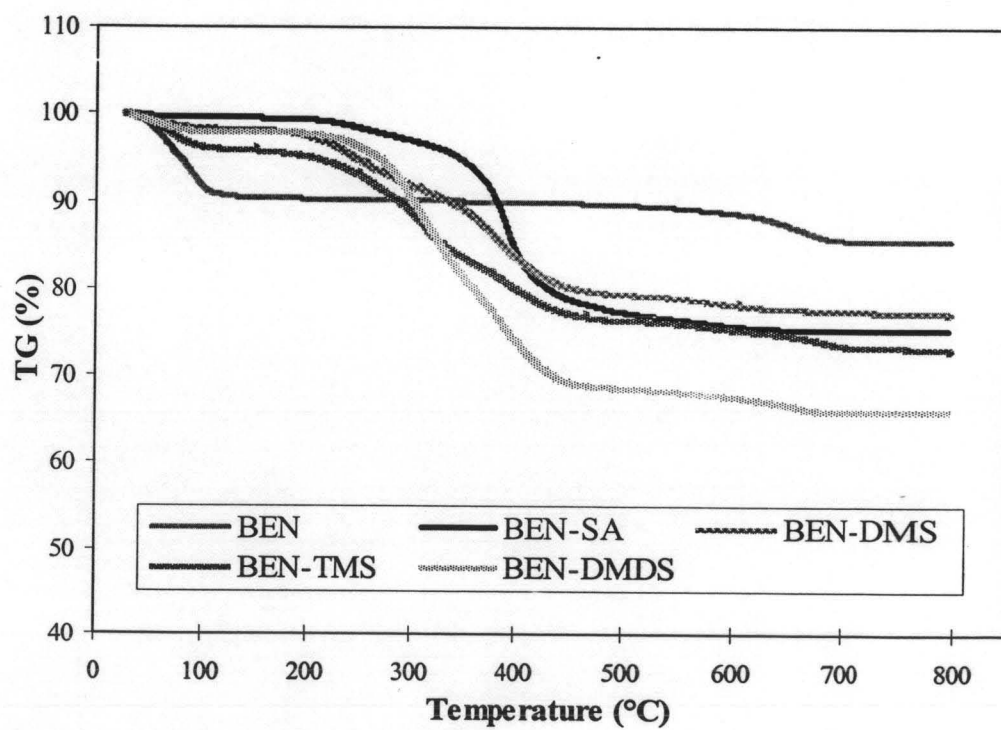


Figure E4 TG thermograms of organo-BENs.

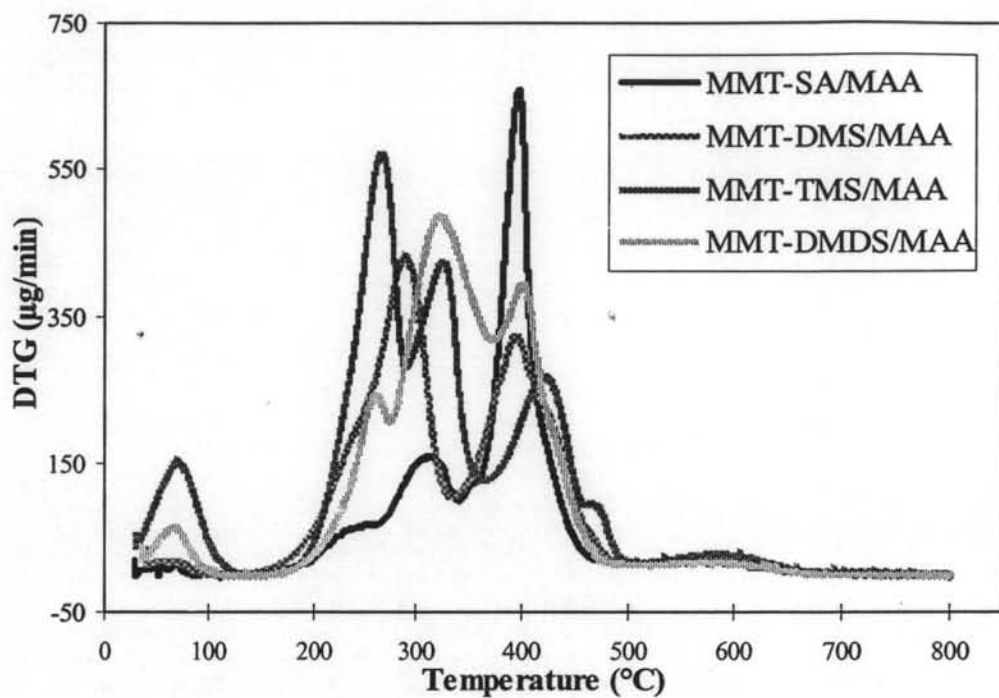


Figure E5 DTG thermograms of modified organo-MMTs.

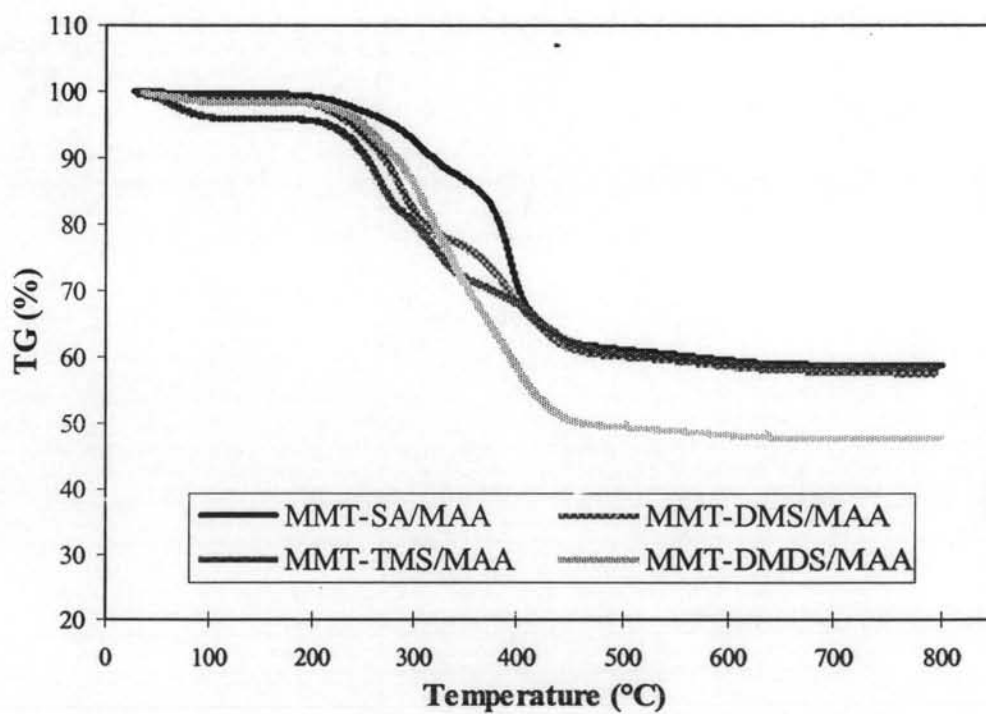


Figure E6 TG thermograms of modified organo-MMTs.

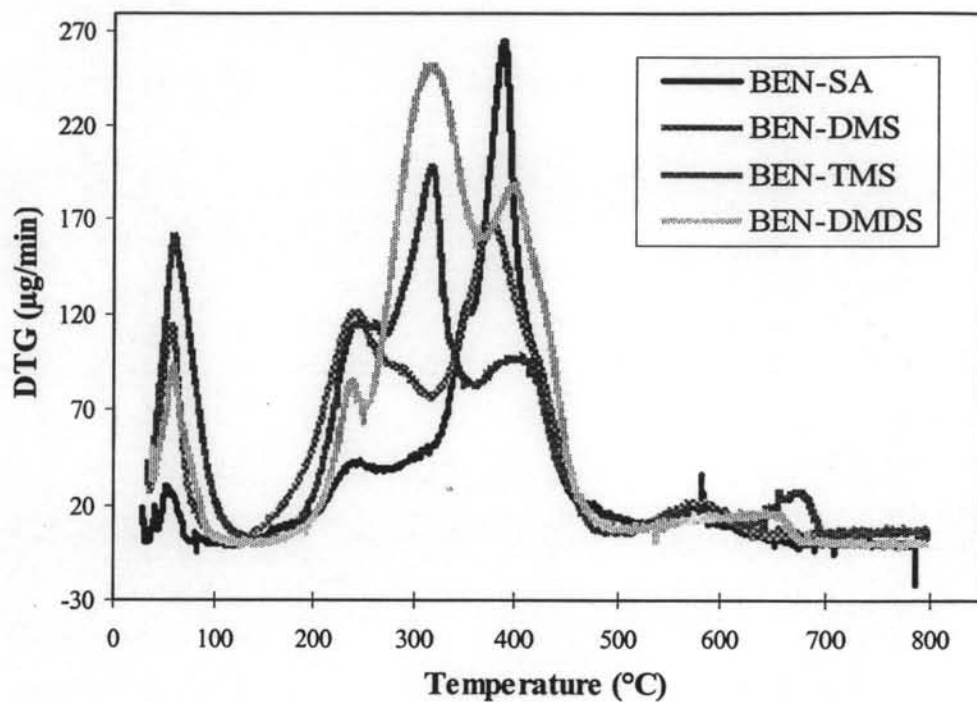


Figure E7 DTG thermograms of modified organo-BENs.

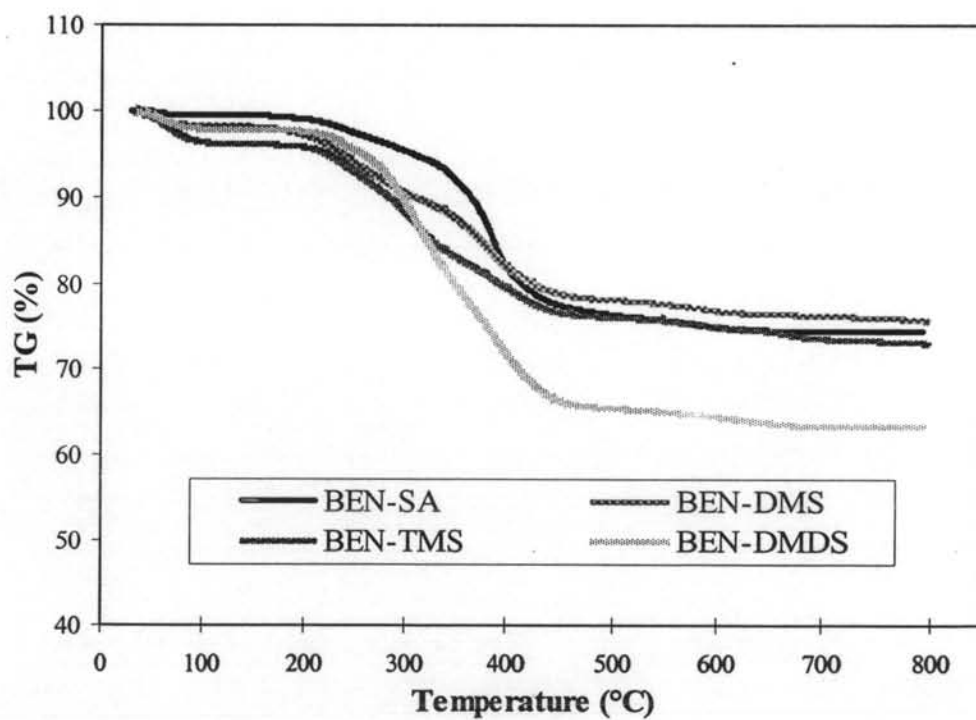


Figure E8 TG thermograms of modified organo-BENs.

Table F1 %Crystallinity of PP/clays nanocomposites

Nanocomposites	ΔH_{DSC} (J/g)		$\Delta H_{100\% \text{ matrix}}$ (J/g)		%Crystallinity	
	MMT	BEN	MMT	BEN	MMT	BEN
PP-SA/MAA 3%	63.197	84.545	65.219	87.250	31.21	41.75
PP-DMS/MAA 3%	61.834	81.531	63.812	84.139	30.53	40.26
PP-TMS/MAA 3%	62.749	78.141	64.756	80.641	30.98	38.58
PP-DMDS/MAA 3%	65.242	79.922	67.329	82.479	32.21	39.46

$\Delta H_{100\% \text{ matrix}}$ was calculated from equation (5)

$$\Delta H_{100\% \text{ matrix}} = \frac{\Delta H_{DSC} * 100}{PP \text{ matrix}} \quad (5)$$

Where:

- $\Delta H_{100\% \text{ matrix}}$ = ΔH value of 100% PP matrix (J/g),
- ΔH_{DSC} = ΔH value from DSC result (J/g), and
- PP matrix = content of PP matrix in nanocomposite (%)

%Crystallinity was calculated from equation (6)

$$\%Crystallinity = \frac{\Delta H_{100\% \text{ matrix}} * 100}{\Delta H_{100\% \text{ matrix}} \text{ of PP } 100\% \text{ crystallinity}} \quad (6)$$

Where:

- %Crystallinity = amount of crystal in nanocomposite (%),
- $\Delta H_{100\% \text{ matrix}}$ = ΔH value of 100% PP matrix (J/g), and
- $\Delta H_{100\% \text{ matrix}} \text{ of PP } 100\% \text{ crystallinity}$ = 209 J/g

Table F2 MFI of PP, PP-PP/DCP, and PP/clays nanocomposites

Materials	1	2	3	4	5	Mean	SD.
PP	10.888	10.916	10.566	10.746	10.862	10.80	0.14
PP-PP/DCP	24.784	24.528	24.504	24.746	24.770	24.67	0.14
PP-MMT- SA/MAA 3%	22.998	22.322	22.384	22.860	23.032	22.72	0.34
PP-MMT- DMS/MAA 3%	15.872	15.734	15.438	16.492	15.436	15.79	0.43
PP-MMT- TMS/MAA 3%	18.758	18.622	19.028	18.686	18.842	18.79	0.16
PP-MMT- DMDS/MAA 3%	23.824	23.254	24.096	23.016	23.806	23.60	0.40
PP-BEN- SA/MAA 3%	23.126	23.512	23.36	23.186	23.374	23.32	0.16
PP-BEN- DMS/MAA 3%	23.252	22.372	22.462	22.282	22.494	22.57	0.40
PP-BEN- TMS/MAA 3%	18.360	18.472	17.162	17.484	17.290	17.75	0.62
PP-BEN- DMDS/MAA 3%	23.516	23.634	23.646	23.490	23.556	23.57	0.06

Table F3 Tensile properties of PP

No.	σ at peak	ϵ at peak	σ at break	ϵ at break	Young's modulus
1	35.966	10.168	22.099	172.574	1965.430
2	35.812	10.010	22.549	235.941	2056.907
3	36.218	9.792	14.942	116.139	2103.468
4	35.816	9.594	19.311	220.594	2103.755
5	35.873	9.802	21.883	201.485	2113.415
Mean	35.94	9.87	20.16	189.35	2068.59
SD.	0.17	0.22	3.18	47.26	61.73

Table F4 Tensile properties of PP-PP/DCP

No.	σ at peak	ϵ at peak	σ at break	ϵ at break	Young's modulus
1	34.736	10.356	22.974	338.614	1870.607
2	35.875	10.099	23.282	416.841	1892.270
3	35.270	10.020	24.008	424.910	1889.597
4	35.341	10.139	24.007	425.506	1988.534
5	34.880	9.723	17.473	373.762	1936.802
Mean	35.22	10.07	22.35	395.93	1915.56
SD.	0.45	0.23	2.76	38.50	47.47

Table F5 Tensile properties of PP-MMT-SA/MAA 3%

No.	σ at peak	ϵ at peak	σ at break	ϵ at break	Young's modulus
1	35.929	8.455	29.045	17.950	2300.195
2	36.357	8.554	30.180	17.871	2256.069
3	36.111	8.515	28.894	18.455	2241.304
4	35.761	8.624	29.755	18.772	2210.425
5	35.801	8.663	7.226	27.149	2199.229
Mean	35.99	8.56	25.02	20.04	2241.44
SD.	0.25	0.08	9.96	3.99	40.03

Table F6 Tensile properties of PP-MMT-DMS/MAA 3%

No.	σ at peak	ϵ at peak	σ at break	ϵ at break	Young's modulus
1	35.063	8.792	26.958	19.931	2377.349
2	35.126	9.010	13.539	23.040	2256.504
3	35.214	9.020	29.972	17.802	2196.094
4	35.071	9.109	15.771	35.465	2183.768
5	35.151	8.931	25.482	25.970	2140.281
Mean	35.13	8.97	22.34	24.44	2230.80
SD.	0.06	0.12	7.25	6.90	91.85

Table F7 Tensile properties of PP-MMT-TMS/MAA 3%

No.	σ at peak	ϵ at peak	σ at break	ϵ at break	Young's modulus
1	35.647	8.950	31.440	15.634	2832.461
2	35.353	9.158	28.631	20.010	2779.897
3	35.632	8.673	30.061	15.475	2776.440
4	35.416	9.030	29.727	18.267	2771.557
5	35.340	8.723	29.387	17.554	2352.966
Mean	35.48	8.91	29.85	17.39	2702.66
SD.	0.15	0.21	1.04	1.90	197.03

Table F8 Tensile properties of PP-MMT-DMDS/MAA 3%

No.	σ at peak	ϵ at peak	σ at break	ϵ at break	Young's modulus
1	35.653	7.851	27.227	15.446	2880.628
2	35.991	8.129	30.010	13.693	2589.835
3	35.961	7.822	27.325	16.980	2452.305
4	35.649	8.079	28.099	16.782	2351.508
5	35.950	8.119	26.766	17.406	2317.113
Mean	35.84	8.00	27.89	16.06	2518.28
SD.	0.17	0.15	1.28	1.51	228.61

Table F9 Tensile properties of PP-BEN-SA/MAA 3%

No.	σ at peak	ϵ at peak	σ at break	ϵ at break	Young's modulus
1	36.629	8.149	30.313	18.465	2316.100
2	36.224	8.376	32.553	14.149	1789.706
3	36.421	8.178	33.022	15.525	1666.118
4	35.644	7.703	31.524	16.119	1643.621
5	36.786	8.02	33.594	13.218	1533.246
Mean	36.19	8.59	31.96	16.04	1667.82
SD.	0.36	0.05	1.19	1.68	114.42

Table F10 Tensile properties of PP-BEN-DMS/MAA 3%

No.	σ at peak	ϵ at peak	σ at break	ϵ at break	Young's modulus
1	36.088	8.653	33.043	15.752	1818.434
2	35.802	8.594	30.097	18.743	1757.713
3	36.765	8.604	32.773	14.218	1620.796
4	36.270	8.545	32.376	15.277	1589.429
5	36.044	8.545	31.526	16.218	1552.748
Mean	36.19	8.59	31.96	16.04	1667.82
SD.	0.36	0.05	1.19	1.68	114.42

Table F11 Tensile properties of PP-BEN-TMS/MAA 3%

No.	σ at peak	ϵ at peak	σ at break	ϵ at break	Young's modulus
1	36.405	8.198	31.741	15.713	2039.530
2	36.268	8.455	30.787	16.010	1952.600
3	35.995	8.030	28.097	18.050	1863.411
4	35.942	8.515	31.029	16.723	1591.010
5	36.161	8.238	31.437	16.277	1575.243
Mean	36.15	8.29	30.62	16.55	1804.36
SD.	0.19	0.20	1.461	0.91	211.41

Table F12 Tensile properties of PP-BEN-DMDS/MAA 3%

No.	σ at peak	ϵ at peak	σ at break	ϵ at break	Young's modulus
1	36.436	8.168	12.533	51.891	2455.601
2	36.089	8.376	16.925	21.366	2256.707
3	36.146	8.218	26.734	14.901	2230.722
4	36.452	8.495	26.027	16.832	2219.432
5	36.548	8.455	27.386	19.228	2189.648
Mean	36.33	8.34	21.92	24.84	2270.42
SD.	0.20	0.14	6.76	15.32	106.28

